Characteristics of the Future Eddying Ocean Circulation

January 2020

Author:
Xun Zhang

1st Supervisor:
Prof. dr. Appy Sluijs
2nd Supervisor:
Prof. dr. ir. Henk A. Dijkstra

Utrecht University

Contents

Abstract

The forced CMIP5 climate model simulations under the RCP scenarios have given us a glimpse of possible future (up to the year 2100) climate states. However, the CMIP5 model results only provide limited information on the variability of crucial climate quantities (e.g. heat transport) since the mesoscale processes can not be represented with the rough resolution (mostly 1° horizontally). Recently, a simulation with a high-resolution (eddying ocean) version of the Community Earth System Model (CESM) has been performed under the RCP8.5 scenario over the period 2000-2100. In this study, we analyze different ocean variables in both the Arctic and the Atlantic basin with the data provided by CESM. Then we further analyze the strength and stability of the Atlantic Meridional Overturning Circulation (AMOC). The results show a continuous weakening trend of the AMOC and suggest the AMOC enters a bistable regime.
KEYWORDS: AMOC, CESM model, Climate change

Chapter 1

Introduction

The Atlantic Meridional Overturning Circulation (AMOC), defined as the zonally-integrated of the current in the Atlantic Ocean, is composed of the warm near-surface northward flow and compensated by the cold southward flow in the deep ocean. As the warm northward flow loses buoyancy in the North Atlantic and sinks to become the southward North Atlantic Deep Water (NADP), the AMOC links to an essential path of poleward ocean heat transport (Lynch-Stieglitz et al. [2007]). The release of the heat from ocean to atmosphere in the North Atlantic makes a significant contribution to the relatively warmer condition in Northwest Europe, which is up to 6°C warmer compared to the same latitude in the North Pacific (Palter [2015]). The change of the AMOC's strength or path can have significant impacts on climate change (Srokosz et al. [2012]). Cheng et al. [2013] detected several regional climate changes which the AMOC can contribute to, such as the African and Indian monsoon rainfall (Zhang and Delworth [2006]), the Ocean CO_2 storage (Key et al. [2004]) and North American and European climate (Sutton and Hodson [2005]).

Open-water deep convection is the main process that feeds the ther-

mohaline circulation, especially what happens in the Labrador and Nordic Seas.(Marshall and Schott [1999]). Here the water mass sinks in response to the winter cooling of the relatively salty surface water, which leads to convective instability and produces the salty and cold NADW. However, Stommel [1961]) analyzed a two-box model and stated there are two types of stable steady-state solutions: active circulation (modern AMOC) and reversed circulation. Since then, many pieces of research have come out and further completed the theory (e.g., Rahmstorf [1996]). Lynch-Stieglitz et al. [2007] pointed the equilibria can be changed from one steady-state to another with the anomalies in the surface freshwater flux. Furthermore, de Vries and Weber [2005] and Weber and Drijfhout [2007] found that the monostable and bistable regimes of the AMOC were well predicted by the sign of Mov, which is defined as the freshwater transport induced by the merional circulation (see the Method part). They found the bistable regime of the AMOC only occurs when the MOC exports freshwater (negative Mov). Since the freshwater export is seen from many observations (e.g., Bryden et al. [2011]; Garzoli et al. [2013]; King and McDonagh [2005]; Weijer et al. [1999]), it suggests the modern AMOC is in a bistable regime. Also, the observation taken by RAPID array shows the average of AMOC strength from April 2004 to February 2017 at 26.5°N is 17.0 Sv, with a 15% weakening trend over the 13-year record length(Weijer et al. [2019]; Smeed et al. [2018]).

There are several models used for the AMOC study, for instance, Phase 5 of the Coupled Model Intercomparison Project (CMIP5). Cheng et al. [2013] analyses ten models from CMIP5 under RCP8.5 simulation and shows 15%-60% weakening of the AMOC strength by the year 2100 compared to the individual models' historical mean state. However, the results of the AMOC strength can be different with various models' resolution in the same simula-

tion. Fuentes-Franco and Koenigk [2019] examines the sensitivity of Arctic freshwater content and transport in three models with different resolutions and shows that less freshwater in the central Arctic Ocean and more in the Kara and Laptev sea with higher model resolutions. It is known that processes on the internal Rossby deformation radius, in particular, eddies, play a crucial role in setting the three-dimensional ocean circulation, both their mean and their variability. Consequently, the low-resolution model results only provide limited information on changes in western boundary currents, overturning circulation, heat transport, and sea level. Therefore, to determine more specific and reliable projections of the future ocean circulation, high-resolution ocean model components are needed. Here we use the high-resolution version of the Community Earth System Model (CESM) to analyze different ocean quantities such as freshwater, salinity, and temperature.

The research question of this paper is how the AMOC strength will change within the freshwater and heat budget change under RCP8.5 CO_2 concentration forcing. The structure of this paper is as follows: first, the Method part will describe the CESM model's simulation and validation in detail, also with the functions used for this research; then, the main character changes in the Arctic and Atlantic basins will be discussed separately in the Results part; finally, I will answer the research question with the explanation of all the results in the Discussion part.

Chapter 2

Methods

2.1 Model Description

The model used in this study is the Community Earth System Model (CESM), which is a fully-coupled, global climate model providing state-of-the-art computer simulations of the Earth past, present, and future climate states. Here we use version 1.04. There are five components coupled with CESM Coupler (CPL7): Community Atmosphere Model (CAM5), Community Land Model (CLM4), Community Ice CodE (CICE4), Parallel Ocean Program (POP2) and Community Ice Sheet Model (Glimmer-CISM).
(`http://journals.ametsoc.org/page/CCSM4/CESM1`).

2.1.1 Model Simulation

There are two model simulations analysed: Representative Concentration Pathway 8.5 (RCP8.5) of CO_2 concentration by the Intergovernmental Panel on Climate Change (IPCC) for its fifth Assessment Report (AR5) in 2014, and the constant CO_2 concentration at year 2000 (CTRL). Figure 2.1 shows the well-mixed carbon dioxide concentration and its radiative forcing (Etmi-

nan et al., 2016). The model is run for 200 years before our research scenario (RCP8.5) and continued for another 100 years.

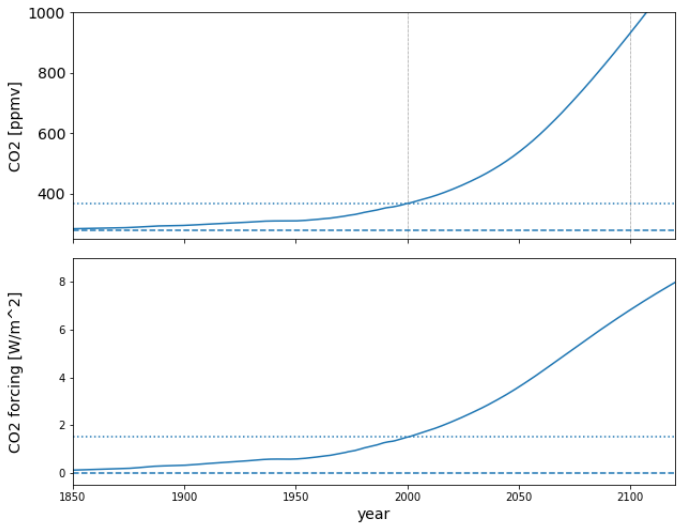

Figure 2.1: Top: Historical CO_2 concentration (up to 2005; solid) and projected CO_2 concentration(from 2005) under RCP8.5 scenario. Bottom: The associated radiative forcing. The horizontal lines represent pre-industrial (lower dashed line) and present (year 2000, higher dashed line) CO_2 concentrations. Figure courtesy of André Jüling

With the high resolution both for the ocean field (0.1°) and the atmosphere field (0.47° × 0.63°), it becomes possible to analyze mesoscale eddy activity, which is an essential component of heat transport. Figure 2.2 shows the time series of the global mean surface temperature (GMST) and the AMOC strength under the two model simulations. Even with the constant CO_2 concentration in the year 2000, the GMST is still keeping increasing while it rises up dramatically under the RCP8.5 scenario. Also, the AMOC is getting weaker continuously for CTRL run and drops significantly for the RCP run.

Figure 2.3 shows the mean SST from 2030 to 2059 results in RCP 8.5 scenario (up), CTRL run(middle) and the difference (bottom). Most regions

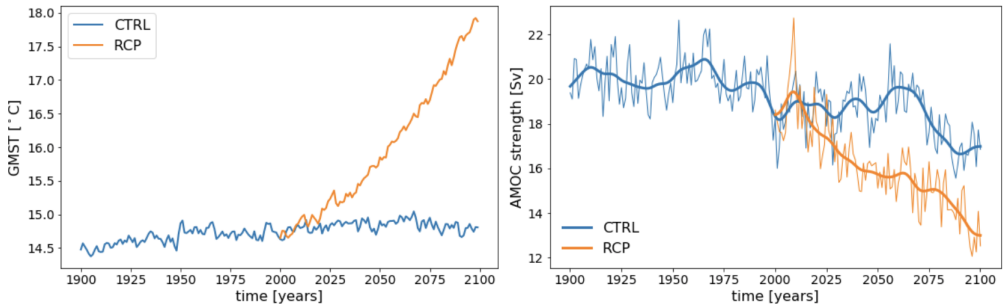

Figure 2.2: Left: global sea surface temperature (GSMT). Right: the AMOC strength with ten-year lowpass filter. The orange line represents CTRL run while the blue line represents RCP scenario.

of the ocean heat up in the RCP scenario compared to the CTRL scenario, except for the North Atlantic due to the weakening of the AMOC strength, which reduces northward ocean heat transport.

2.1.2 Model Validation

We validated the model's Arctic sea ice area and the sea surface temperature. Figure 2.4 shows that the Arctic sea ice area in the summer is much less than HadiSST observation both in the RCP run and CTRL run. During Northern Hemisphere's winter (Figure 2.4 left), there is a sharp transition for RCP run, while both the CTRL run and the observation change slightly. In Northern Hemisphere's summer (Figure 2.4 right), the sea ice area in our simulation is minimal. The sea ice even disappears after 2080 in RCP run, while there is still much remained in reality, though starts declining from 1980 to the present day. The reason of the asymmetry is that sea ice is so sensitive to sea surface temperature and atmospheric temperature, only a slightly increase than freezing point can result in colossal sea ice loss. The first 200 years of our model run are based on the forcing given by the CO_2 concentration in the year 2000, which is higher than reality. With the high

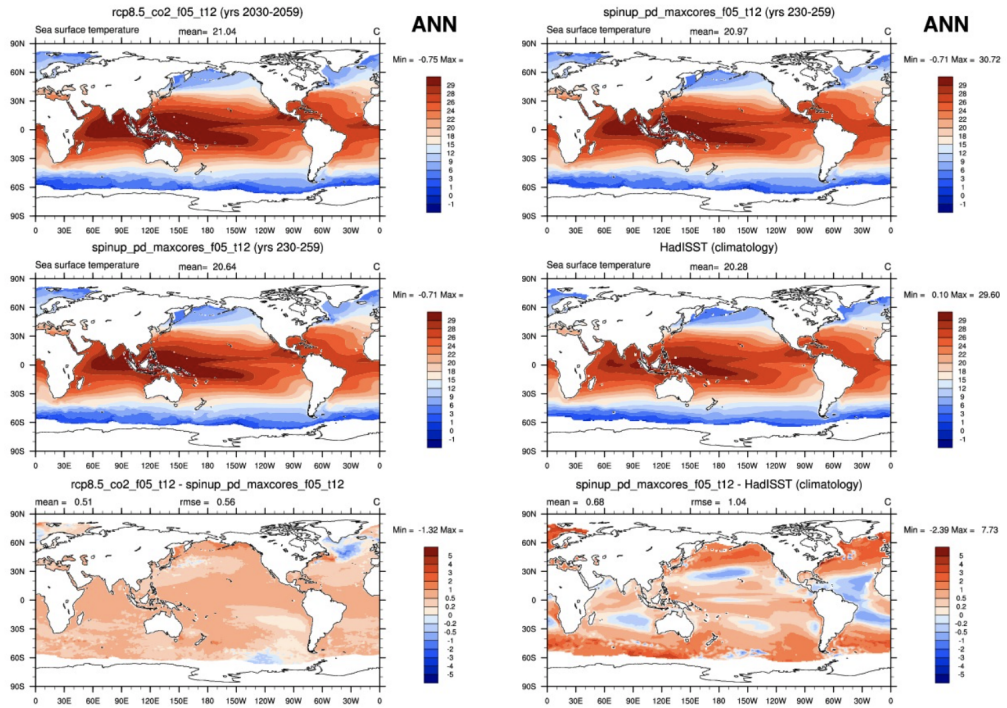

Figure 2.3: Mean sea surface temperature from 2030 to 2059, Left: RCP scenario (up), CTRL(middle), and the difference between them (bottom); Right: CTRL(up), observation (middle), the difference (bottom)

resolution, such high CO_2 concentration results in a higher Atmosphere and surface ocean temperature, also higher ocean heat transport into the Arctic basin.

Figure 2.3 shows the difference of mean SST between the CTRL simulation and the observation. The model results expect lower SST at subtropical gyres and higher sea surface temperatures at high latitude regions. For the Atlantic basin, lower SST is expected in whole tropical areas.

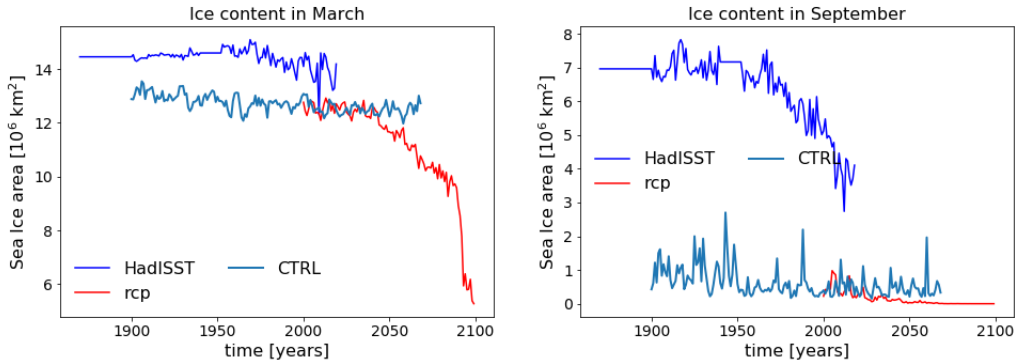

Figure 2.4: Arctic sea ice area time series. Left: sea ice area in March (Northern hemisphere's summer); Right: in September. The dark blue line, the green line, and the red line represent the observation, CTRL simulation, and RCP simulation

2.2 Model Analysis

2.2.1 AMOC strength

The AMOC strength is defined as the volume transport at 26 °N from surface water to 1000m depth (Stepanov et al. [2016]):

$$\psi(z) = \int_{X_w}^{X_e} \int_{-H}^{Z} v(x,z)dzdx$$

Where X_w and X_e are western and eastern boundaries, and z is the vertical coordinate, H is 1000 meter depth which is the no motion level.

2.2.2 M_{ov} and M_{az} Calculation

The calculation for M_{ov} and M_{az} components are defined as:

$$M_{ov} = -\frac{1}{S_0} \int \bar{v}[\langle S(z) - S_0 \rangle]dz$$

$$M_{az} = -\frac{1}{S_0} \int \overline{v'(z)S'(z)} dz$$

Where S_0 is a reference salinity calculated by the average of the salinity over the section, the overbar and the brackets denote zonal integration and zonal averaging, respectively, and v' and S' are deviations from zonal means (de Vries and Weber [2005]). Both M_{ov} and M_{az} are calculated at 34 °S, which is the southern boundary of the Atlantic Ocean.

The overturning component M_{ov} represents the net freshwater flux carried by the MOC. For negative values of M_{ov}, the MOC exports the freshwater. The azonal part M_{az} serves both the export of freshwater via subtropical gyre and the flows inputting from the Indian Ocean and the Drake Passage. In equilibrium, the freshwater budget of the Arctic and Atlantic basin can be closed as followed:

$$[E - P - R] = M_{ov} + M_{az} + M_{diff} + M_{BS}$$

Where E, P, and R represent the net basin-integrated evaporation, precipitation, and continental runoff separately; The other terms represent the diffusion at 34°S and freshwater transport through Bering Strait to the Arctic, respectively.

Chapter 3

Results

3.1 Change of Arctic

3.1.1 Sea Ice

Sea ice in the polar regions has essential impact on global climate system. First of all, the ice-albedo feedback mechanism makes sea ice very sensitive to the change of surface temperature: higher surface temperature →less ice →less reflected solar energy back to atmosphere →higher surface temperature. Second, the melting of the sea ice provides freshwater resource importing to the ocean, and transport to the North Atlantic, which can impact the AMOC's strength and stability. So we checked the sea ice reaction in our simulations. As mentioned in the Model Validation part, the Arctic sea ice area in model results does not fit that in the observation well (Figure 2.4), while some exciting patterns still can be concluded. A dramatic reduction of sea ice area in winter happens from 2080 to the end of the RCP simulation. Instead of the impact of the positive feedback, the rapid decline can be explained by the seasonal asymmetry in the ice distribution. Arctic win-

ter sea ice is spread out more homogeneously compared to that in summer, which means that once the water temperature is warmer than the freezing point in winter, the tiny loss of sea ice extent from one winter can result in a Dramatic drop to the next (*S. Bathiany, 2016*). Figure 3.1 also shows the spread of sea ice loss from one month to the next and from one winter to another. In the year 2010 and 2025, a notable ice area decline happens in the summer (dashed lines), while there is just a slight decreasing in the winter (solid lines). And once the Arctic basin becomes ice-free in the summer, a huge crash of sea ice happens later and later (after the year 2070).

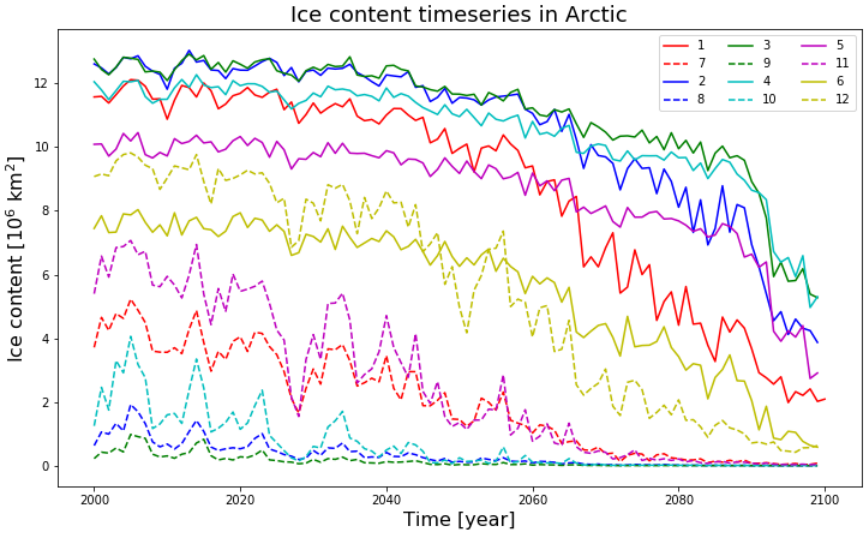

Figure 3.1: Monthly change of the Arctic sea ice area for RCP senario

Figure 3.2 shows the spatial sea ice concentration trend of the Arctic Ocean. The most sea ice loss happens at the outer boundary of the Arctic basin in the winter (left, March), including Bering Strait and Fram Strait. The declining trend in the summer (right, September) is not obvious since less ice left in summer at the beginning of RCP simulation already.

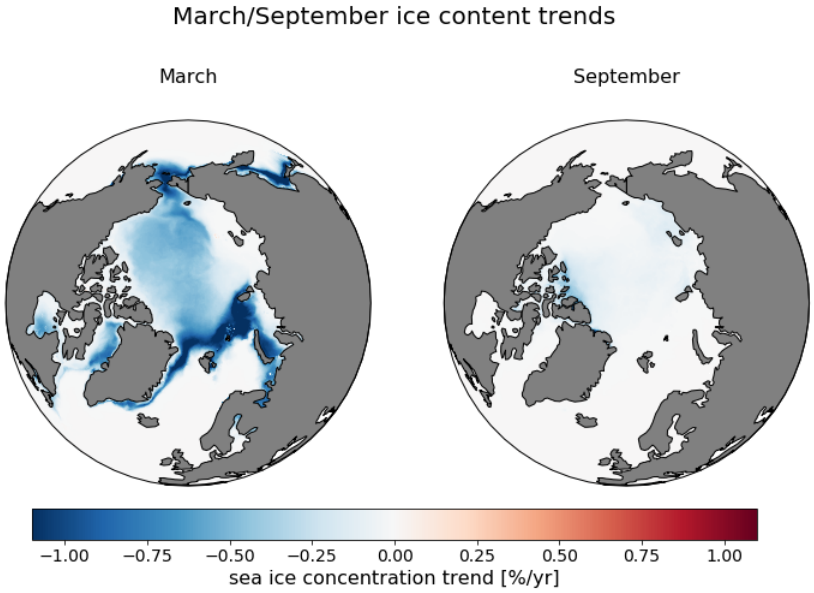

Figure 3.2: Arctic sea ice concentration trend. Left: in March; Right: in September. Note the small trends in September are due to the small sea ice content in CESM model

3.1.2 Ocean Stratification

With the notable sea ice area decline in the Arctic ocean, ocean stability also changes a lot (Figure 3.3). Here we use static stability to describe the stability of the Arctic Ocean. Figure 3.3 shows the anomaly change of spatial-averaged static stability over the Arctic basin. The sign of static stability's value is always negative, so the increasing anomaly value in the graph indicates the weakening of the stratification. The static stability at surface layer (above 50m depth) becomes less negative, the surface column becomes less stable, which indicated a large amount of ice melting and freshwater accumulation; A strong stratification occurs at the upper layer (50-200 m depth); And again a weakening stratification happens at the intermediate water column (200-700 m depth), and a slight increasing at the deep ocean (700-3000 m, note the range of color bar is 100 times less than the upper graph).

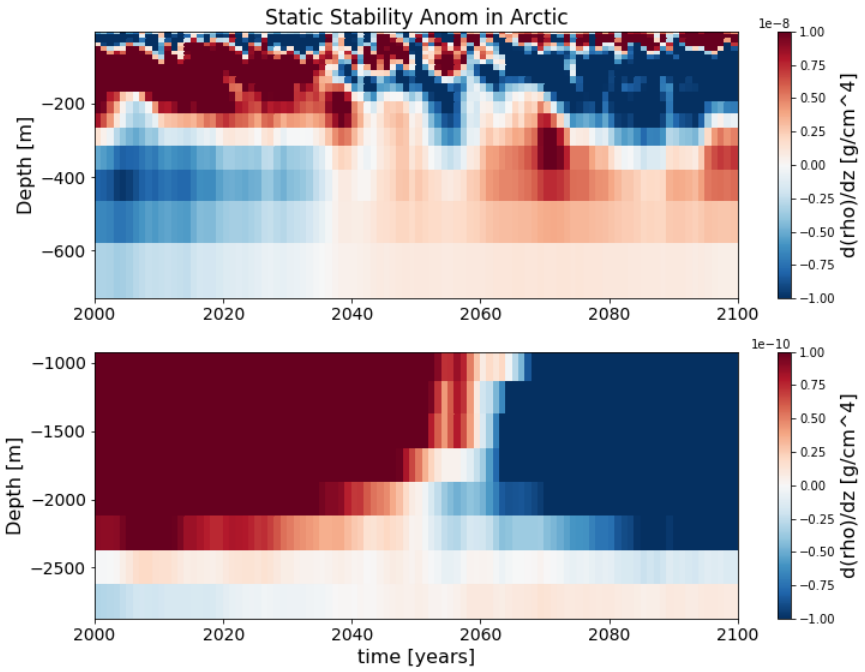

Figure 3.3: Static stability anomaly with respect to the mean over the year 2000-2100 in Arctic. The value of Static stability itself is always negative, the positive trend indicates the stratification is getting weaker. Note the scale of the second graph is 100 times less than the first one

To understand if the change of the ocean stability is dominated by the change of temperature or salinity, we analyze the salinity and the temperature change in the Arctic. Figure 3.4 shows the spatial-averaged salinity change, the left graph shows the mean salinity of the first ten years, the last ten years, and all one hundred years separately; the right graph shows the salinity anomaly change. Both of the graphs indicated that at the surface layer (above 200 meters), the water becomes fresher, while at the intermediate layer (100 to 750 meters), the water becomes saltier. Figure 3.5, however, shows the warming trend happening all the water column above 1500 meter depth.

Combined the Figure 3.3, 3.4 and 3.5, the stratification at the interme-

diate water depth between 100 and 300 meters due to both the fresher and warmer conditions. In contrast, the deeper layer between 300 and 700 meters becomes less stable, dominated by the increase of salinity.

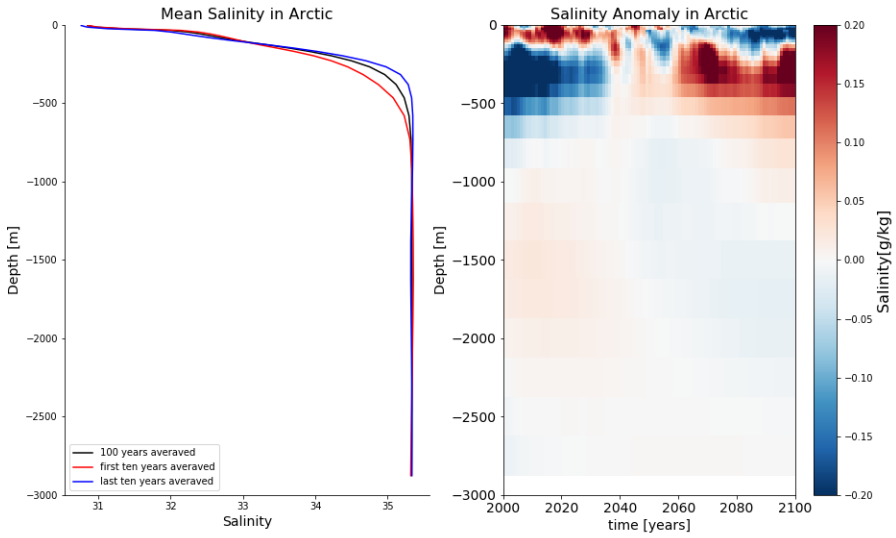

Figure 3.4: Salinity profile in Arctic. Left: The mean salinity in Arctic. Right: Salinity anomaly with the respect to the mean value over 100 years

3.1.3 Transport across Sections

With rapid sea ice and stability changes in Arctic, some changes also occur on the interaction between Arctic and Atlantic Ocean. We select two sections, which are the main transport paths between the Arctic and the Atlantic, to anaylse several parameters' transport: Fram Strait and the section from Svalbard to Russia (S-R)(Figure 3.6).

For Fram Strait, the heat transport profile (Figure 3.7, first line) shows the southward heat transport through East Greenland Current (EGC) is increasing. The strengthened southward heat transport compensates the stronger

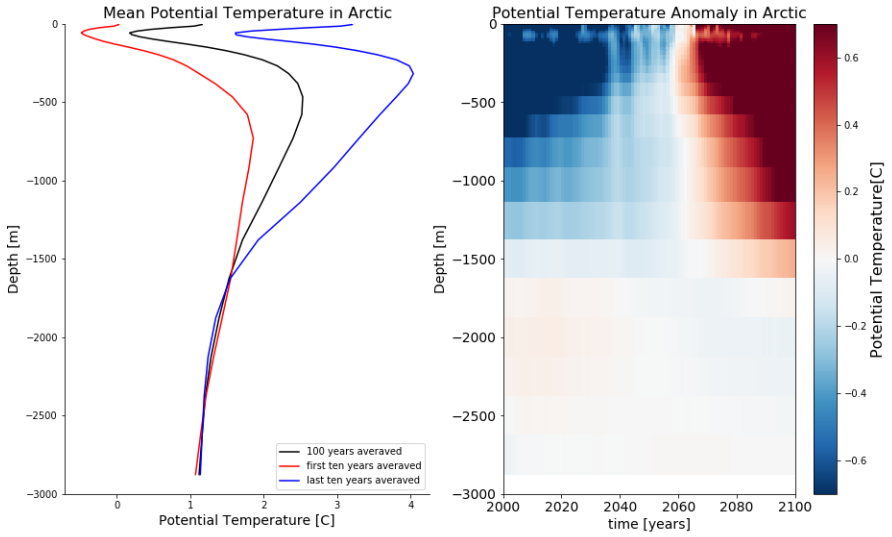

Figure 3.5: Temperature profile in Arctic. Left: The mean temperature in Arctic. Right: Temperature anomaly with the respect to the mean value over 100 years

northward heat transport carried by West Spitsbergen Current (WSC), so the total heat transport (Figure 3.7(1,3)) doesn't change much on the amplitude. However, it fluctuates sharper after the year 2040. The velocity profile (Figure 3.7, second line) shows the structure change of EGC and WSC: the surface and the deep layer of EGC is weakening while the intermediate layer of it strengthens; the eastern part of WSC has a notable decline while the western part is getting stronger. The temperature profile (Figure 3.7, third line) indicates that the whole water column heats up, and the most vigorous heating happens at the surface and the intermediate layer. Also, the time-series of heat content (Figure 3.7(3,3)) shows the accumulation of heat content becomes more notable after the year 2040. The last three graphs of Figure 3.7 reveal that an increase in eddy activities and stronger eddy energy transport after the year 2040.

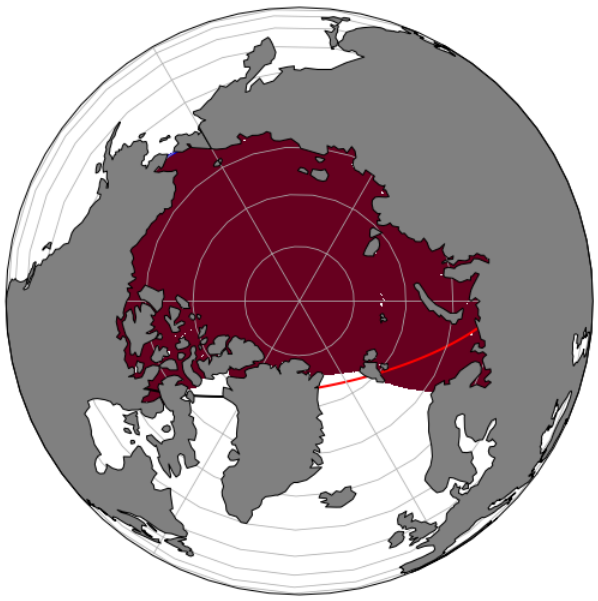

Figure 3.6: Arctic Ocean range (dark red contour) and the selected sections (red lines): Fram Strait and the section S-R.

For the second section, the heat transport profile (Figure 3.8, first line) shows both the northward and southward heat transport are enhanced, and in total more heat transport into the Arctic basin through this section (Figure 3.8(1,3)). However, the velocity of flows is getting slower, which results in the decline of northward volume transport (Figure 3.8, second line). Combined with the dramatic temperature rising at all water depths, the enhanced northward heat transport is resulted by the warmer condition. The water heats up so much that even a weakening northward volume transport can bring more heat compared to the beginning. The last three graphs of Figure 3.8 shows that the direction of eddy heat transport changes from poleward to southward.

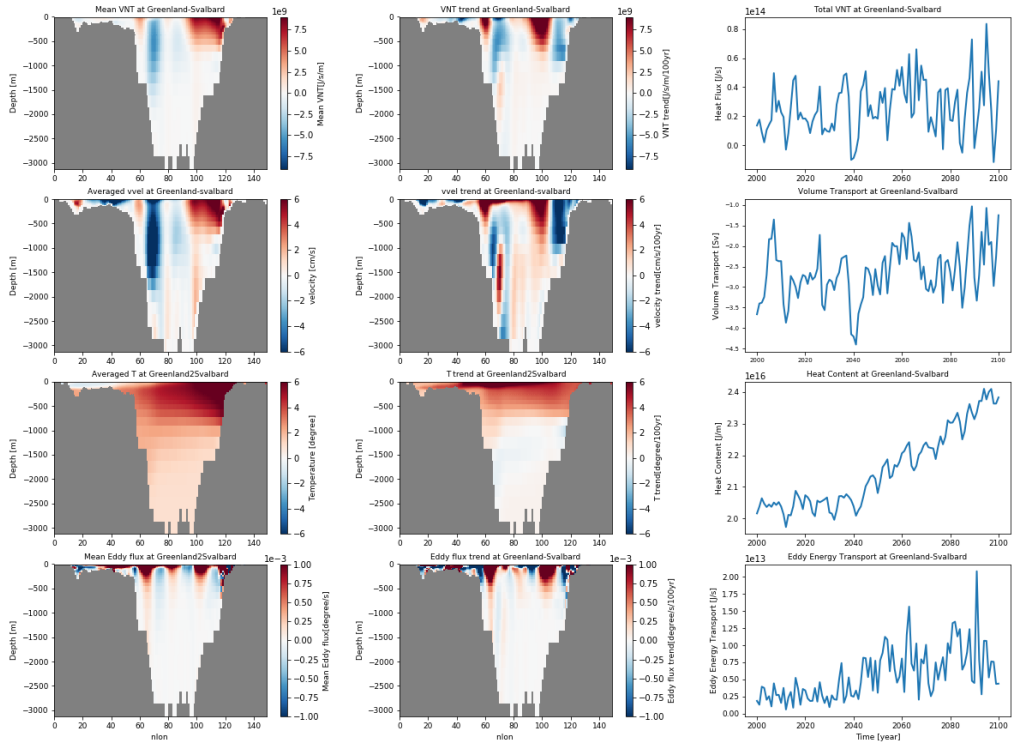

Figure 3.7: Section profile and time-series of heat, volume, eddy transport and heat content at Fram Strait. Top to bottom: Heat transport; Velocity; Temperature; Eddy energy transport. Left to right: Mean value over 100 years, red indices northward transport; the trend, red indices increasing trend; the time-series of: Heat transport, Volume transport, Heat content, Eddy energy transport

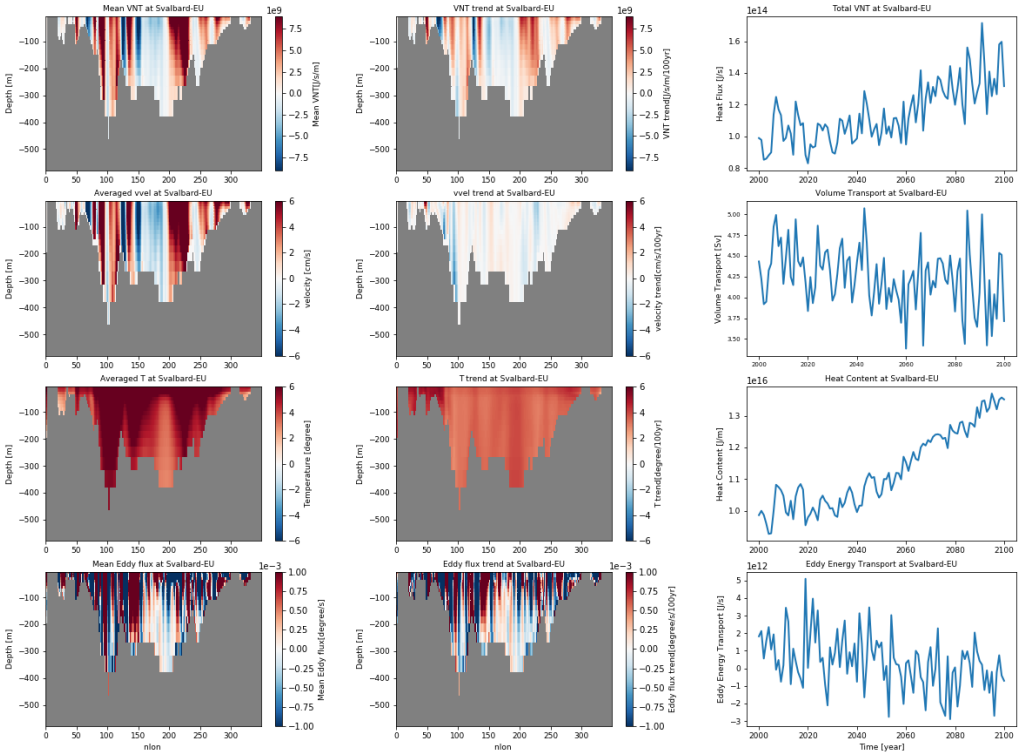

Figure 3.8: Section profile and time-series of heat, volume, eddy transport and heat content at S-R. Top to bottom: Heat transport; Velocity; Temperature; Eddy energy transport. Left to right: Mean value over 100 years, red indices northward transport; the trend, red indices increasing trend; the time-series of: Heat transport, Volume transport, Heat content, Eddy energy transport

3.2 Changes of Atlantic

3.2.1 AMOC strength change

The Atlantic meridional overturning circulation (AMOC), defined as the zonally-integrated component of surface and deep currents in the Atlantic Ocean, consists of the near-surface northward warm flow, compensated by the southward cold flow at depth (*M. SrokoSz*). The AMOC is an essential component of the climate system because of the transport of heat from

southern hemisphere across the equator, that even reaches to northwest Europe. As the AMOC is sinking down and turning southward at high latitude of North Atlantic due to the abundant loss of heat, the changes in Arctic can impact the strength and/or path changes of AMOC.

Here we define the strength of AMOC as the volume transport in 26 °N from surface water to 1000m depth and plot the time-series over 100 years RCP run from 2000 to 2100 (Figure 3.9), combined with a ten-year low-pass filter to remove annual variability. The result indicates a continuous weakening of AMOC, around 0.06 Sv per year.

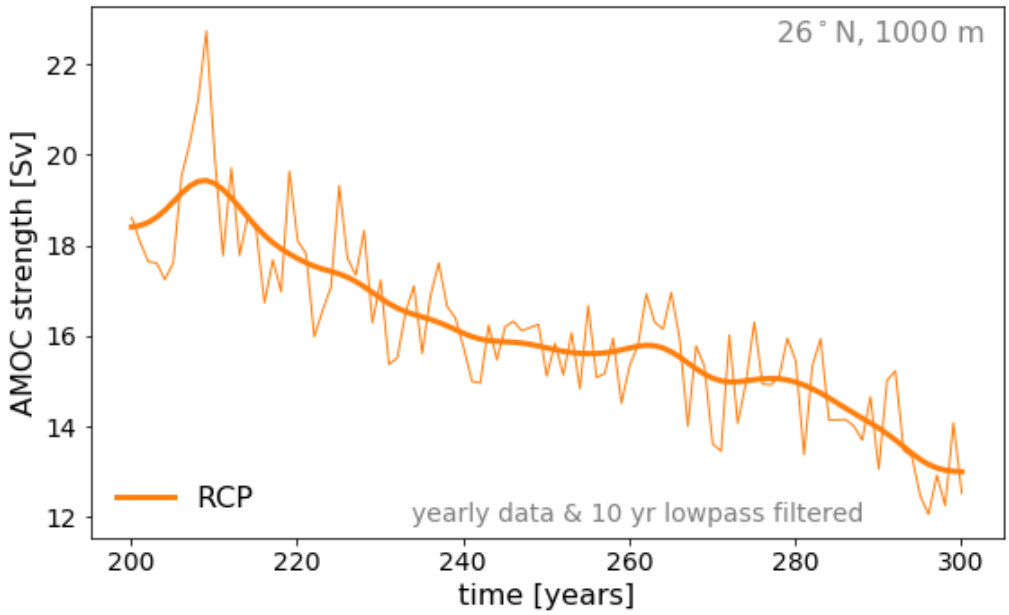

Figure 3.9: AMOC strength time-series. Thin line: year-averaged data; Thick line: 10 year low-pass filtered

3.2.2 Atlantic heat and salt budget

In order to figure out the reason behind the weakening of the AMOC, we close the Atlantic basin and calculate the salt and the heat budget over 100

years of the RCP run (Figure 3.10and3.11). Positive value means transport into the Atlantic basin while negative value represents output transport. The salt flux between atmosphere and Atlantic is transformed from the freshwater flux between them (Precipitation - Evaporation + Continental Runoff) with reference salinity. The salt budget result (Figure 3.10) shows the main salt resource comes from the Labrador Sea and the atmosphere, while the most of salt ends up to the Greenland sea and the Southern Ocean. There is an enhance of the salt transport of both the input from the Labrador Sea and the output to the Greenland sea. Surprisingly, the salt input from atmosphere doesn't change much. The sum of all these salt fluxes (Figure 3.10, purple line) shows that generally the Atlantic is getting salter. It is worth noting that the result of the salt budget could have errors due to the chosen value of reference salinity. Also the freshwater fractions depend on the choice of reference salinity in a non-linear way (Schauer and Losch [2019]), which makes the result of atmosphere salt transport more ambiguous.

For the heat budget part (Figure 3.11), the overall transport is from the southern hemisphere to the northern hemisphere, from the atmosphere to the ocean. The heat input from the atmosphere has an obvious increase due to the radiative forcing (Figure 2.1). However, even with the rise of global mean ocean temperature, the heat transports at the Labrador Sea and the Southern Ocean are still weakening, indicating a weakening trend of the currents' strength there.

3.2.3 Stability of the AMOC

To further analyze the stability of the AMOC, we calculate the meridional overturning freshwater transport and azonal component: M_{ov} and M_{az}, at the southern border of the Atlantic at 34°S (see Model Analysis) (Figure

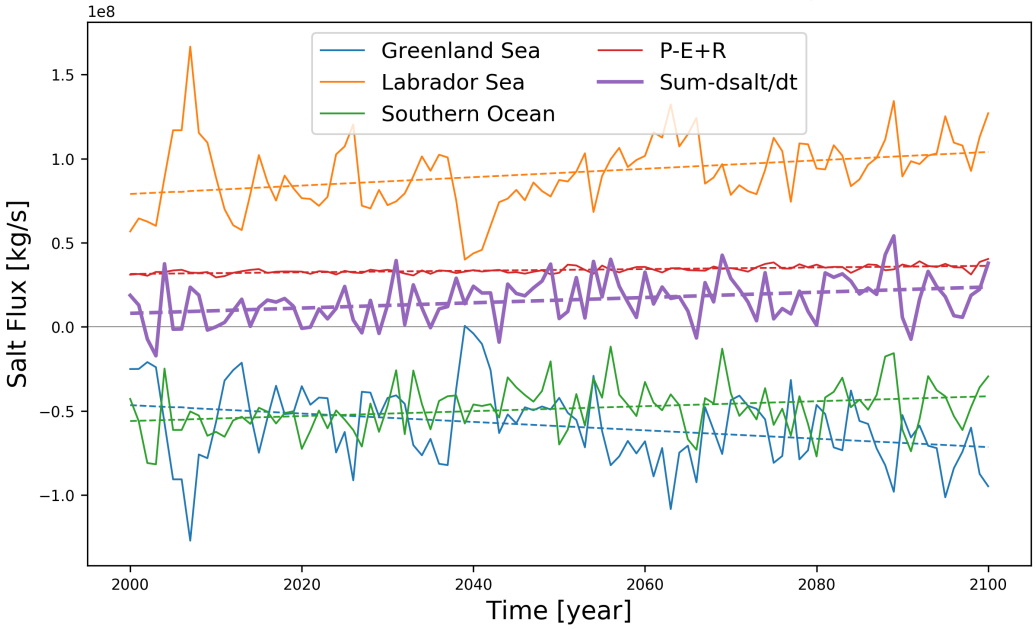

Figure 3.10: Atlantic Salt Budget

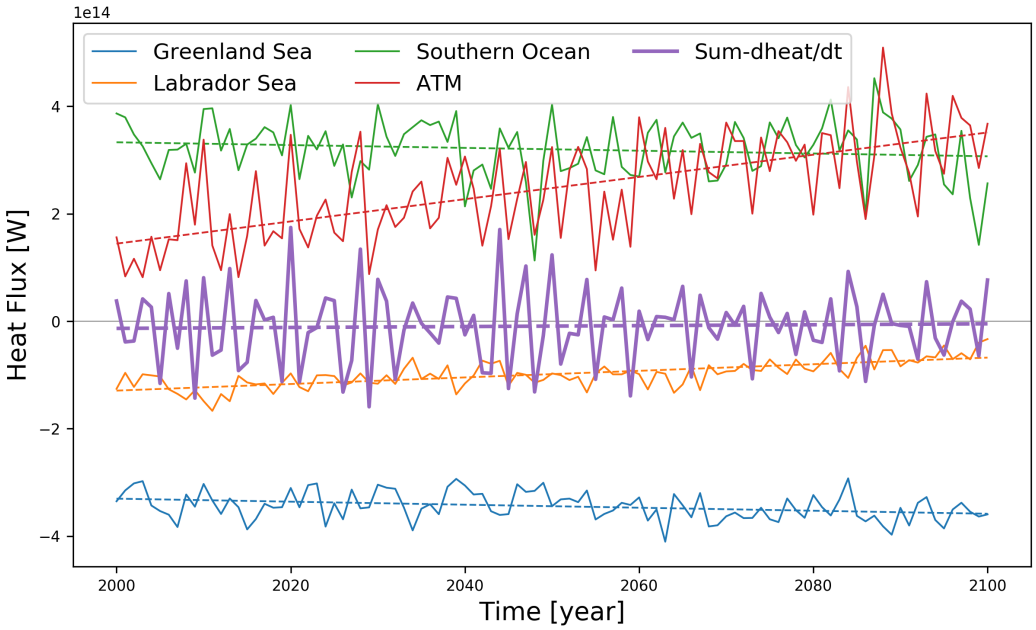

Figure 3.11: Atlantic Heat Budget

3.12). The result shows there is a continuous decrease of M_{ov} value from +0.1Sv to -0.075 Sv within 100 years, compensated by the increase of the M_{az}. The notable event is the sign of M_{ov} changes to negative after the year 2060, the AMOC turns to export freshwater.

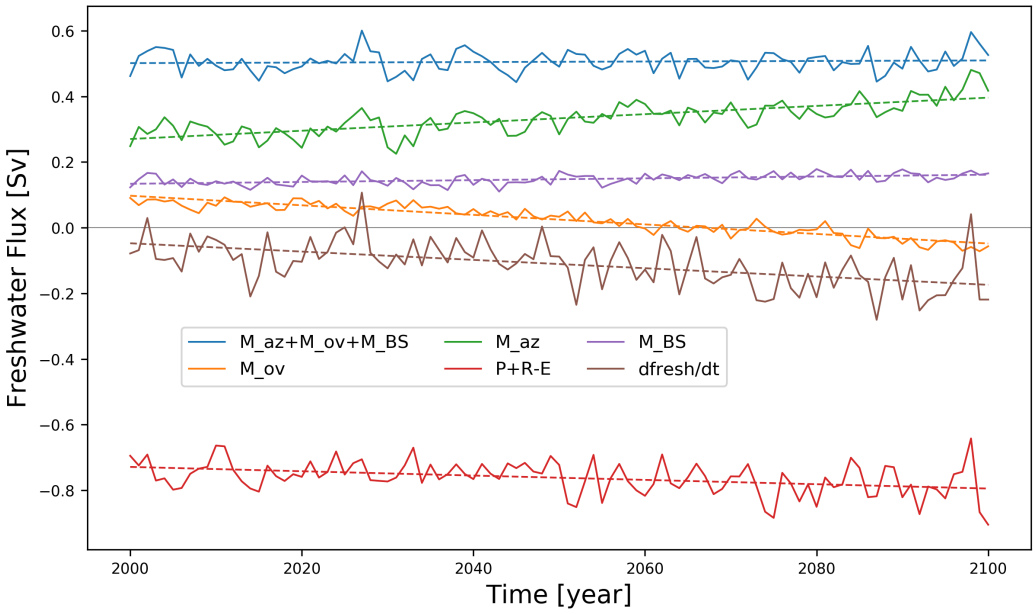

Figure 3.12: Freshwater budget over whole Atlantic and Arctic basin

Fig 3.12 also shows the salter condition of the whole Arctic and Atlantic basin. To figure out the exact regions of the salinity change, we plot the Fig 3.13, the upper graph shows the salinity trend over 100 years in surface layer (upper 5m), while the bottom graph shows that in deeper layer (10 to 500m). For the surface layer, most of the areas in Atlantic is getting salter, while a notable freshening happens in the Labrador Sea and the Sub-polar Gyre. The freshening trend can be explained by both the freshwater input from sea ice melting and the weakening of the AMOC, which carries less salt mass to this region. A similar salinity trend pattern can be found below the surface (Figure 3.13, second graph), though the freshen trend at the sub-polar gyre

is weaker. These salinity changes tend to weaken the stratification of the subtropical gyres and enhance that in the Labrador Sea, make the North Atlantic Deep Water (NADW) harder to form, in other words, make the AMOC even weaker.

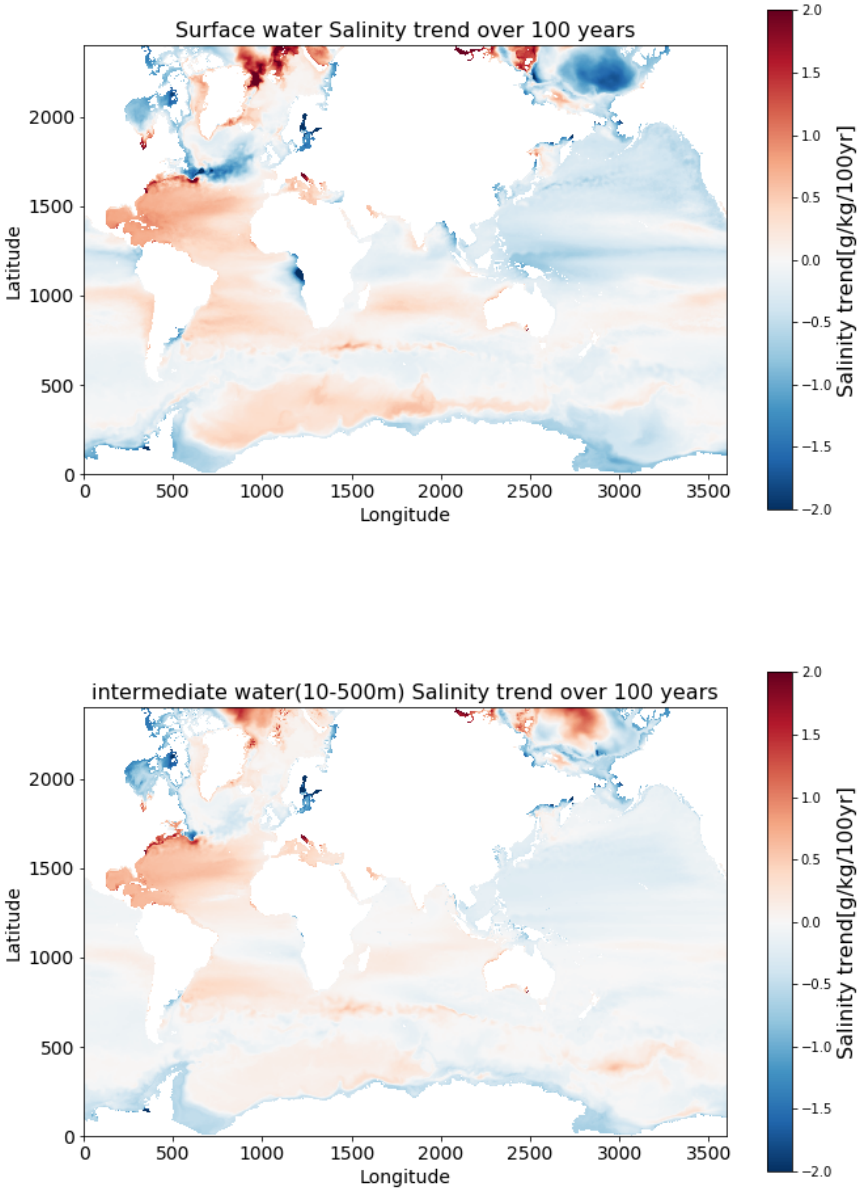

Figure 3.13: Salinity trend pattern. top: top layer (5m); bottom: deeper depth(10˜500m)

Chapter 4

Discussion

4.1 Change of Arctic

First we analyse the changes of different ocean quantities in the Arctic. We care about this basin because the atmosphere and SST here might has a huge increase with the effect of polar amplification, which could have an essential impact on, for instance, sea ice extent and ocean stratification. Those changes could result in an amount of freshwater input to the North Atlantic, increasing surface buoyancy and reducing the formation of NADW.

The results show that the sea ice extent in the Arctic is quite small in our RCP simulation, especially during the Northern Hemisphere summer. The difference between the model sea ice and observation is because of the 200 years run before the RCP run, which is based on the CO2 concentration in the year 2000. The higher radiative forcing associated with higher CO2 concentration heats the Arctic, resulting in less sea ice than observation. When the sea surface temperature is so high that no ice forms in the winter, a tiny loss of sea ice in the summer can result in a significant collapse of sea ice in the next summer (Figure 2.4, the year 2080).

With the ice-albedo effect of the sea ice loss, the exposed seawater heats up efficiently, resulting in more sea ice loss. On the one hand, abundant seawater heats up by exposure to the atmosphere from the sea ice melting, leading to the accumulation of heat content in the upper-layer water, results in the enhanced stratification of Arctic intermediate water (Figure 3.3). On the other hand, this freshwater flows along the Hudson Bay and Fram Strait into Labrador sea and subpolar gyre, increasing the surface buoyancy by decreasing the water salinity and then damping the formation of the North Atlantic Deep Water (Figure 3.13).

The analysis over two sections (Figure 3.7 and 3.8) shows the exchange between the Arctic and the Atlantic also changes. The East Greenland Current is getting shallower from 2000 meter depth in the first 30 years to 1500 meter in the last 30 years. Meanwhile, the northward West Spitsbergen Current as a compensation to the East Greenland Current also becomes shallower, and spread wider at the upper layer (above 500 meter depth) (Appendix Figure 5.1). With the changing structure of these two currents, the volume transport becomes less negative, in other word, slower southward volume transport. Also the eddy activities are playing more important role on energy transport in Fram Strait. The volume transport in the section S-R is also reduced, the decline might be explained by the weaker AMOC that less water can reach to this section (Figure 3.8 and Appendix 5.2.

4.2 Change of Atlantic

The results show the weakening trend of the AMOC strength in the 21st century by 35%. The continuous weakening of the AMOC can be explained by the positive feedback: On the one hand, the melting of Arctic sea ice

provides abundant freshwater into Atlantic, the increased water buoyancy makes the formation of North Atlantic Deep Water hard, which reduces the source of the AMOC. On the other hand, the weaker AMOC brings less high-salinity water mass from southern hemisphere, which makes the subpolar gyre even fresher.

Then we closed the salt and heat budget of the Atlantic basin (Figure 3.10 and 3.11). The Atlantic basin gains salt from Labrador Sea and atmosphere (loss freshwater), and transports the salt into the Greenland Sea and the Southern Ocean. Both the salt transports into the Greenland Sea and out the Labrador Sea are enhanced, the salt flux from atmosphere does not change much. In total, the Atlantic Ocean has a positive net salt flux (see also Appendix5.3 and 5.4). For the heat budget, the general direction of it is from Southern Ocean to the northern hemisphere and from atmosphere to the ocean. The Atlantic has a positive net heat transport, the ocean heat content is accumulated.

To analyze the stability of the AMOC, we closed the freshwater budget of the Arctic and Atlantic as a whole, based on the method provided by de Vries and Weber [2005] (Figure 3.12). The result the M_{ov} component keeps decreasing and the sign changes after the year 2060, indicting that the AMOC from importing freshwater changes to export water, also from monostable regime to bistable regime. The decreased M_{ov} component is compensated by the increase of M_{az}. The Barotropic Stream Function results (Fig 4.1) show a slowdown of South Atlantic Gyre Circulation, which might result from the weaker wind stress and result in lower salt import, higher freshwater import, in another word. It explains the rise of M_{az} magnitude in compensation to the decrease of M_{ov} component.

We expect to see more disturbance of the AMOC strength with the

changed-sign M_{ov}, which indicates the AMOC becomes bistable. We remove the long-term trend and seasonal signal of monthly-averaged AMOC strength, try to see more extreme fluctuations happening after the year 2060 (Figure 4.2). The result shows a slight increase of the standard deviation after the year 2060. However, the time scale of our results is too short (only 100 years), it is hard to find significant disturbance in our model.

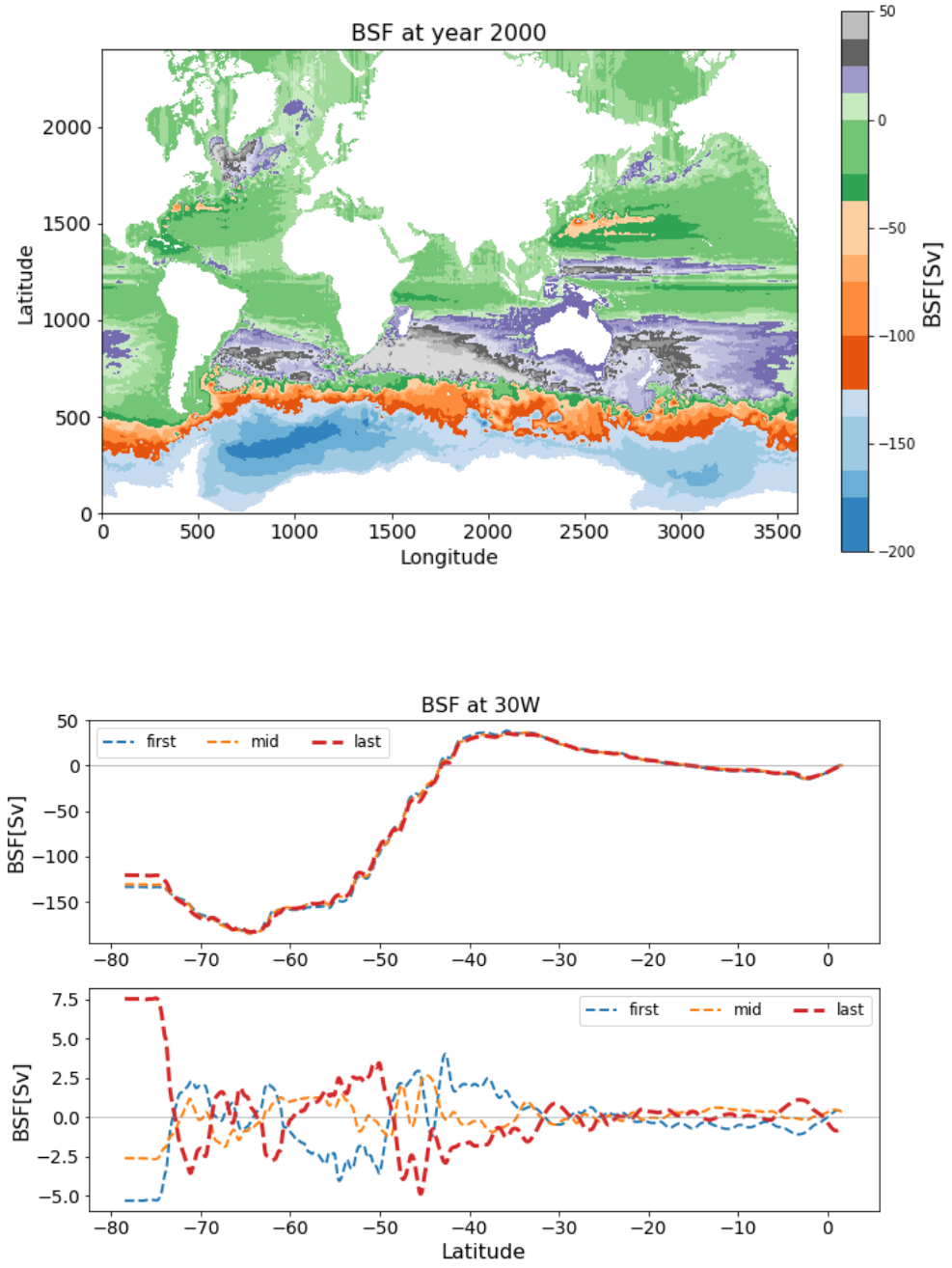

Figure 4.1: Barotropic stream function. First graph: the BSF in the year 2000; Second graph: the first, the middle, and the last 30 year averaged BSF; Third graph: the 30 year averaged BSF minus whole time averaged BSF

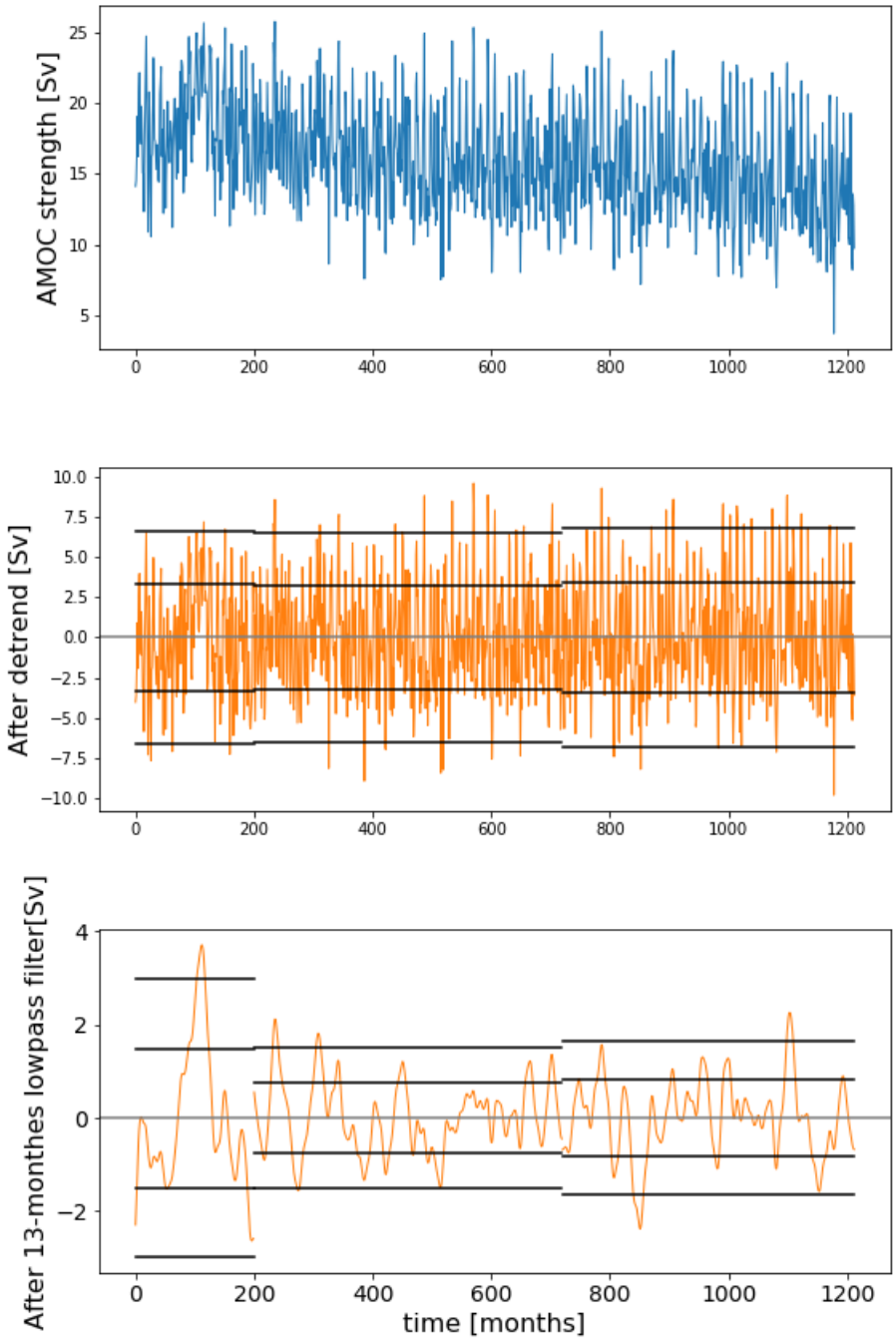

Figure 4.2: AMOC analysis. First graph: Monthly averaged AMOC strength; Second graph: after linear detrended; Third graph: After 13 months lowpass filtered. The black solid lines present the standard deviation and 2 times of the standard deviation around the mean. Note the standard deviations are calculated in three periods, and the first period should be ignored because the model needs to adapt the abrupt RCP8.5 forcing.

Chapter 5

Summary

With rapid Arctic sea ice melting under RCP8.5 simulation, an amount of freshwater transport into the subpolar region of the Atlantic, increasing the surface buoyancy, and damping the formation of the North Atlantic Deep Water, resulting in the weakening of the AMOC. Meanwhile, the weakened AMOC brings less high-salinity water mass to the subpolar region, which enhances the stratification. This positive feedback makes the AMOC strength weaker continuously. The sign of M_{ov} changes to be negative after the year 2060, indicating the AMOC enters a bistable regime. It is also proved by the detrended analysis: the fluctuation of the AMOC becomes shaper after the year 2060. However, the evidence is not so convincing since the increase of standard deviation is small. One reason is the M_{ov} theory is based on the equilibrium state, while our model is under the RCP8.5 forcing simulation; another reason is that the time scale of our data is too short to observe the significant change of the AMOC's fluctuation. So for further study, one possible direction is to clarify the reason why the sign of the M_{ov} changes; another direction might is to find a more convincing method to test the stability of the AMOC.

Appendix

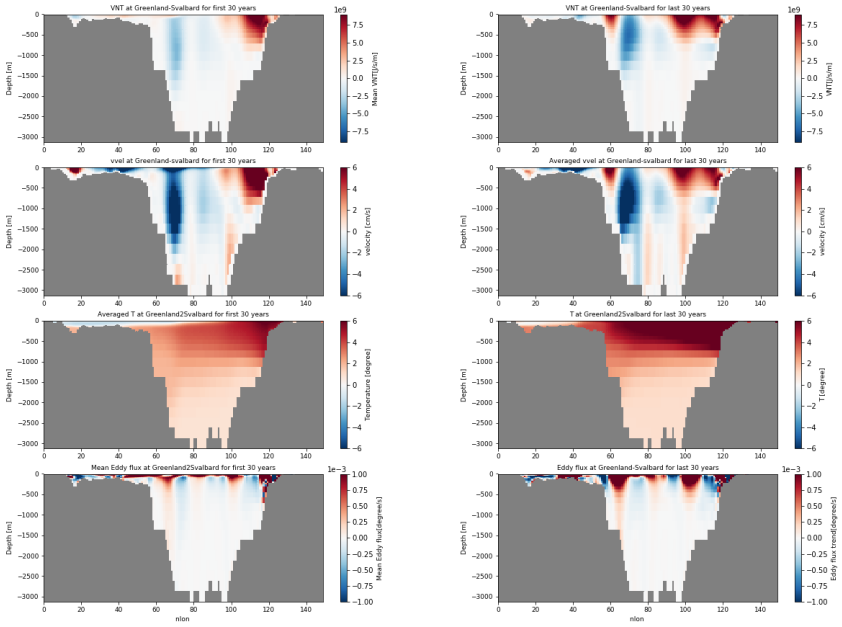

Figure 5.1: The first 30 year and the last 30 year averaged transport in Fram Strait. Top to bottom: Heat transport; Velocity; Temperature; Eddy energy transport. Left to right: Mean value over 100 years, red indices northward transport; the trend, red indices increasing trend.

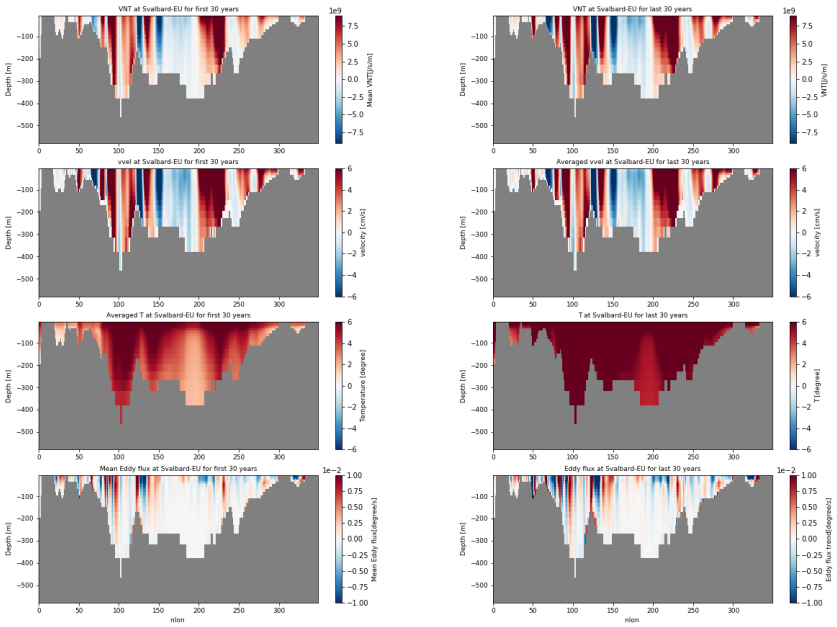

Figure 5.2: The first 30 year and the last 30 year averaged transport in section S-R. Top to bottom: Heat transport; Velocity; Temperature; Eddy energy transport. Left to right: Mean value over 100 years, red indices northward transport; the trend, red indices increasing trend.

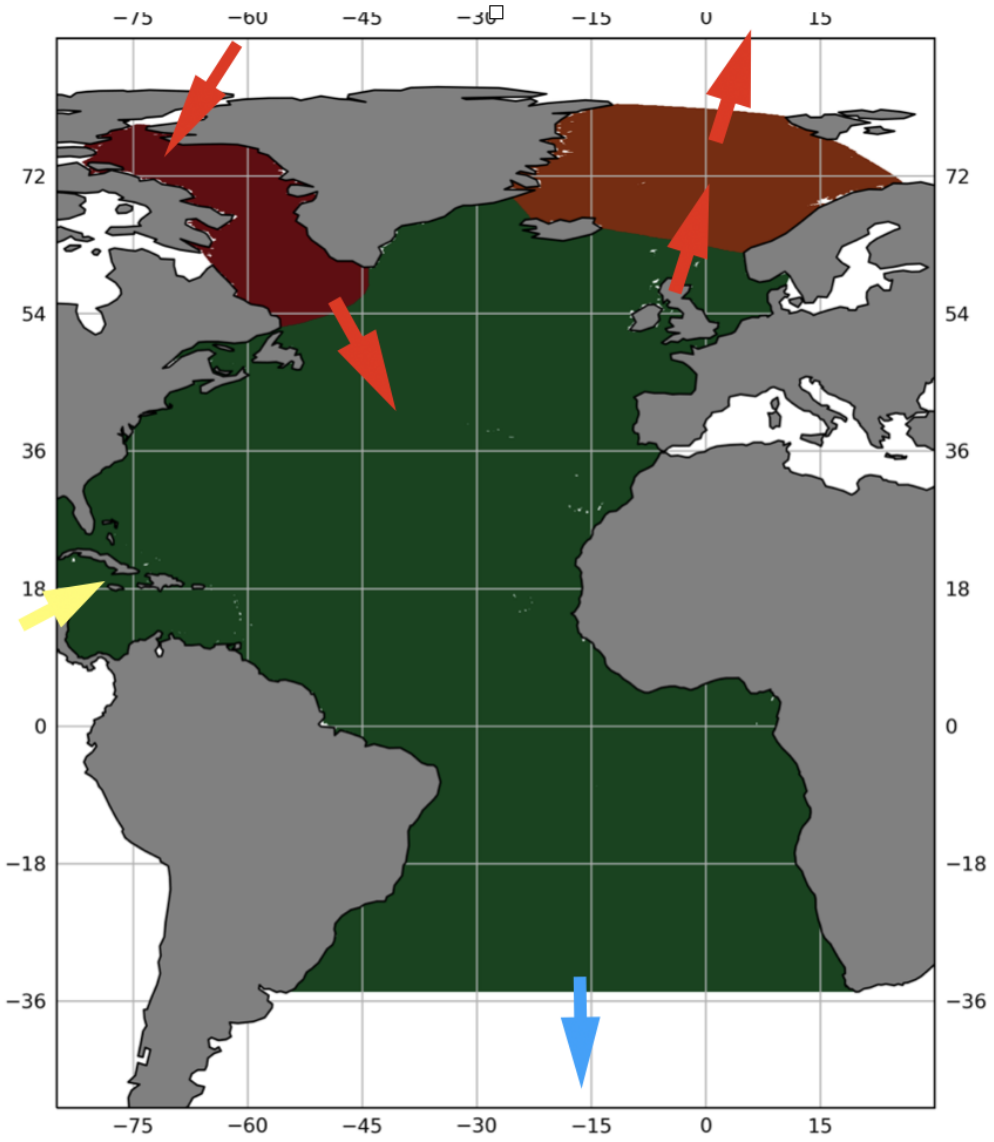

Figure 5.3: Salt flux budget. Red: enhanced transport; Blue: weaken transport; Yellow: the transport doesn't change much. The direction of the arrows indicates the direction of the transport

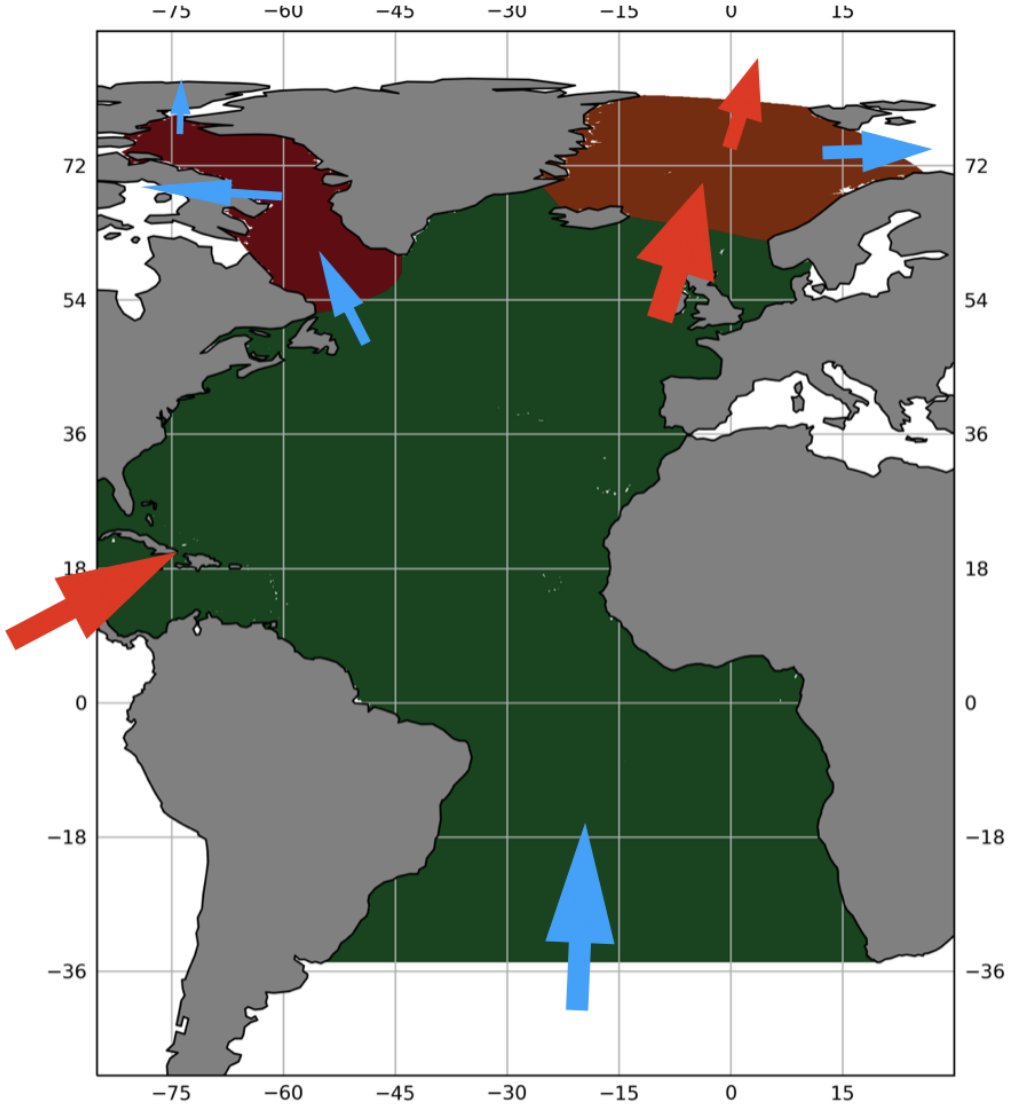

Figure 5.4: Heat flux budget. Red: enhanced transport; Blue: weaken transport; Yellow: the transport doesn't change much. The direction of the arrows indicates the direction of the transport

Bibliography

Harry L. Bryden, Brian A. King, and Gerard D. McCarthy. South Atlantic overturning circulation at 24Â°S. *Journal of Marine Research*, 69(1):39–56, 2011. ISSN 00222402. doi: 10.1357/002224011798147633.

Wei Cheng, John C.H. Chiang, and Dongxiao Zhang. Atlantic meridional overturning circulation (AMOC) in CMIP5 Models: RCP and historical simulations. *Journal of Climate*, 26(18):7187–7197, 2013. ISSN 08948755. doi: 10.1175/JCLI-D-12-00496.1.

Pedro de Vries and Susanne L. Weber. The Atlantic freshwater budget as a diagnostic for the existence of a stable shut down of the meridional overturning circulation. *Geophysical Research Letters*, 32(9):1–4, 2005. ISSN 00948276. doi: 10.1029/2004GL021450.

Ramón Fuentes-Franco and Torben Koenigk. Sensitivity of the Arctic freshwater content and transport to model resolution. *Climate Dynamics*, 53 (3):1765–1781, 2019. ISSN 14320894. doi: 10.1007/s00382-019-04735-y.

Silvia L. Garzoli, Molly O. Baringer, Shenfu Dong, Renellys C. Perez, and Qi Yao. South Atlantic meridional fluxes. *Deep-Sea Research Part I: Oceanographic Research Papers*, 71:21–32, 2013. ISSN 09670637. doi: 10.1016/j.dsr.2012.09.003.

R. M. Key, A. Kozyr, C. L. Sabine, K. Lee, R. Wanninkhof, J. L. Bullister, R. A. Feely, F. J. Millero, C. Mordy, and T. H. Peng. A global ocean carbon climatology: Results from Global Data Analysis Project (GLODAP). *Global Biogeochemical Cycles*, 18(4):1–23, 2004. ISSN 08866236. doi: 10.1029/2004GB002247.

Brian A. King and Elaine L. McDonagh. Decadal changes in ocean properties revealed by ARGO floats. *Geophysical Research Letters*, 32(15):2–5, 2005. ISSN 00948276. doi: 10.1029/2005GL023145.

Jean Lynch-Stieglitz, Jess F. Adkins, William B. Curry, Trond Dokken, Ian R. Hall, Juan Carlos Herguera, Joël J.M. Hirschi, Elena V. Ivanova, Catherine Kissel, Olivier Marchal, Thomas M. Marchitto, I. Nicholas McCave, Jerry F. McManus, Stefan Mulitza, Ulysses Ninnemann, Frank Peeters, Ein Fen Yu, and Rainer Zahn. Atlantic meridional overturning circulation during the last glacial maximum. *Science*, 316(5821):66–69, 2007. ISSN 10959203. doi: 10.1126/science.1137127.

John Marshall and Friedrich Schott. Open-ocean convection: Observations, theory, and models. *Reviews of Geophysics*, 37(1):1–64, 1999. ISSN 87551209. doi: 10.1029/98RG02739.

Jaime B. Palter. The Role of the Gulf Stream in European Climate. *Annual Review of Marine Science*, 7(1):113–137, 2015. ISSN 1941-1405. doi: 10.1146/annurev-marine-010814-015656.

S. Rahmstorf. On the freshwater forcing and transport of the Atlantic thermohaline circulation. *Climate Dynamics*, 12(12):799–811, 1996. ISSN 14320894. doi: 10.1007/s003820050144.

Ursula Schauer and Martin Losch. âFreshwaterâ in the Ocean is Not a Useful Parameter in Climate Research. *Journal of Physical Oceanography*, 49(9):2309–2321, 2019. ISSN 0022-3670. doi: 10.1175/jpo-d-19-0102.1.

D. A. Smeed, S. A. Josey, C. Beaulieu, W. E. Johns, B. I. Moat, E. Frajka-Williams, D. Rayner, C. S. Meinen, M. O. Baringer, H. L. Bryden, and G. D. McCarthy. The North Atlantic Ocean Is in a State of Reduced Overturning. *Geophysical Research Letters*, 45(3):1527–1533, 2018. ISSN 19448007. doi: 10.1002/2017GL076350.

M. Srokosz, M. Baringer, H. Bryden, S. Cunningham, T. Delworth, S. Lozier, J. Marotzke, and R. Sutton. Past, present, and future changes in the atlantic meridional overturning circulation. *Bulletin of the American Meteorological Society*, 93(11):1663–1676, 2012. ISSN 00030007. doi: 10.1175/BAMS-D-11-00151.1.

Vladimir N Stepanov, Doroteaciro Iovino, Simona Masina, Andrea Storto, and Andrea Cipollone. Methods of calculation of the atlantic meridional heat and volume transports from ocean models at 26.5Â° n. *Journal of Geophysical Research: Oceans*, 121(2):1459–1475, 2016.

HENRY Stommel. Thermohaline Convection with Two Stable Regimes of Flow. *Tellus*, 11, 1961. ISSN 16642155. doi: 10.1159/000448962.

Rowan T. Sutton and Daniel L.R. Hodson. Ocean science: Atlantic Ocean forcing of North American and European summer climate. *Science*, 309 (5731):115–118, 2005. ISSN 00368075. doi: 10.1126/science.1109496.

Susanne L. Weber and Sybren S. Drijfhout. Stability of the Atlantic Meridional Overturning Circulation in the last glacial maximum climate. *Geophysical Research Letters*, 34(22):1–5, 2007. ISSN 00948276. doi: 10.1029/2007GL031437.

W. Weijer, W. Cheng, S. S. Drijfhout, A. V. Fedorov, A. Hu, L. C. Jackson, W. Liu, E. L. McDonagh, J. V. Mecking, and J. Zhang. Stability of the Atlantic Meridional Overturning Circulation: A Review and Synthesis. *Journal of Geophysical Research: Oceans*, 124(8):5336–5375, 2019. ISSN 21699291. doi: 10.1029/2019JC015083.

Wilbert Weijer, Wilhelmus P.M. De Ruijter, Henk A. Dijkstra, and Peter Jan Van Leeuwen. Impact of interbasin exchange on the Atlantic overturning circulation. *Journal of Physical Oceanography*, 29(9):2266–2284, 1999. ISSN 00223670. doi: 10.1175/1520-0485(1999)029⟨2266:IOIEOT⟩2.0.CO;2.

Rong Zhang and Thomas L. Delworth. Impact of Atlantic multidecadal oscillations on India/Sahel rainfall and Atlantic hurricanes. *Geophysical Research Letters*, 33(17):1–5, 2006. ISSN 00948276. doi: 10.1029/2006GL026267.